Dalton Transactions

Accepted Manuscript

ROYAL SOCIETY OF CHEMISTRY

www.rsc.org/dalton

Dalton Transactions

ARTICLE

Gel-assisted Crystallization of $[Ir_4(IMe)_7(CO)H_{10}]^{2+}$ and $[Ir_4(IMe)_8H_9]^{3+}$ clusters derived from Catalytic Glycerol Dehydrogenation

Received 00th January 20xx,
Accepted 00th January 20xx

DOI: 10.1039/x0xx00000x

www.rsc.org/

Liam S. Sharninghausen,[a] Brandon Q. Mercado,[a] Robert H. Crabtree,[a] David Balcells*[b] and Jesús Campos*[a†]

The two title clusters were formed during iridium-catalyzed glycerol dehydrogenation and display a remarkably high NHC content. They were crystallized in either agarose or polyethylene oxide gel matrices, while more conventional crystallization techniques proved unsuccesful. Cluster $[Ir_4(IMe)_8H_9]^{3+}$, with a net charge of +3, was only crystallizable with a polyoxometalate Keggin trianion. The crystal packing of this intercluster compound is discussed. Computational studies position the iridium hydrides and provide insights into the bonding.

Introduction

There is growing interest in low valent transition-metal clusters beyond the classic carbonyl series.[1,2] Here, we report two clusters stabilized by NHC ligands, both characterized crystallographically. Crystallography is a key means of cluster characterization[3] but it can be hard to obtain suitable crystals. In this paper we also describe two gel methods for obtaining crystals of these clusters for which conventional methods failed.

Although a number of clusters have proved to be effective precatalysts,[4] or identified as resting states during catalysis[5] or even proposed as active species,[6] most are catalyst deactivation products. In such cases, their structures may suggest possible countermeasures against deactivation.[7] For example, catalytically inactive iridium dimers,[8] trimers[9] and even tetramers[10] are formed in the deactivation of $[Ir(PR_3)(L)(cod)]^+$ (cod = cyclooctadiene) hydrogenation catalysts, leading to the adoption of bulky ligands L to slow deactivation. In general, structural authentication of multimetallic species derived from catalysis can be a difficult task due to the small amounts of catalyst employed, the complexity of the crude mixtures and the nature of the resulting clusters, all of which can disfavor crystallization.

We now describe the use of aqueous (agarose) and organic (polyethyleneoxide, PEO) gel matrices as powerful tools to access crystals of the title hydride- and NHC-rich (NHC = N-heterocyclic carbene) clusters formed in catalytic dehydrogenation-isomerization of glycerol (Scheme 1).[11] Gel platforms slow down crystallization and provide a truly diffusive medium, avoiding convection and sedimentation.[12,13] Hydrogels are routinely used in protein and macromolecule crystallography,[14] but their application to organic and inorganic molecular compounds has been much more limited.[15] Similarly, organic based gel matrices have recently been developed as powerful tools for crystallization of small molecules in different organic media, but this technique has not yet become popular in synthetic organic or inorganic chemistry. After many unsuccessful efforts using common crystallization techniques to access the title clusters, we were only able to grow crystals using the appropriate gel matrices and, in the case of $[Ir_4(IMe)_8H_9]^{3+}$, also by the right choice of the counteranion ($[PW_{12}O_{40}]^{3-}$).

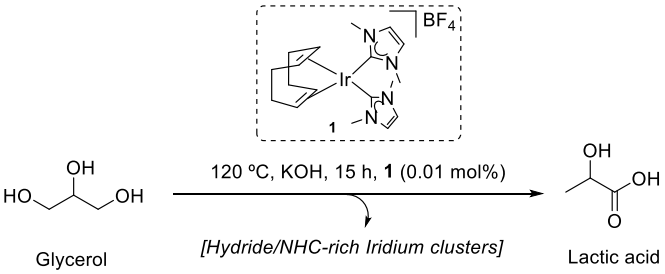

Scheme 1. Iridium-catalyzed glycerol dehydrogenation to lactic acid.

Results and Discussion

Synthesis and Characterization of Iridium Clusters

In studies of our previously described H-transfer precatalyst[16] $[Ir(cod)(IMe)_2]BF_4$ (**1**) (IMe = 1,3-dimethylimidazol-2-ylidene) for the conversion of glycerol to lactic acid,[11] we succeeded in isolating a

[a] Yale University 225 Prospect Street, New Haven, Connecticut 06520 (USA).
[b] Department of Chemistry, University of Oslo Centre of Excellence in Theoretical & Computational Chemistry (CTCC) N-0315 Oslo (Norway).

E-mail: jesus.camposmanzano@yale.edu; david.balcells@kjemi.uio.no
† Present address: Inorganic Chemistry Laboratory, Department of Chemistry, University of Oxford, South Parks Road, Oxford OX1 3QR, UK.
Electronic Supplementary Information (ESI) available: [experimental procedures, spectroscopic, computational and crystallographic details]. See DOI: 10.1039/x0xx00000x

novel 'bow-tie' shaped $[Ir_6(IMe)_8(CO)_2H_{14}]^{2+}$ cluster (**2**),[17] containing eight NHC ligands and 14 metal hydrides (Figure 1, left). During iridium catalyzed glycerol dehydrogenation (40 h, 120 ºC, 0.8 mL of a 1:1 mixture of glycerol/H_2O, 30 equiv. KOH relative to **1**) we observed a plethora of signals in the hydridic region of the ^1H NMR spectra of crude reaction mixtures, beyond those derived from **2**. Motivated by this fact and by the remarkable structural features displayed by **2**, we sought to isolate and characterize further iridium hydride species formed during the reaction.

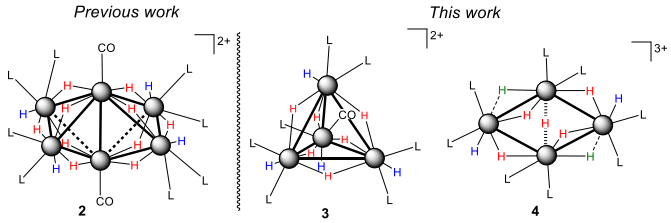

Figure 1. Hydride and NHC-rich iridium clusters previously reported (**2**, left) and presented in this work (**3** and **4**, right). L = IMe and grey spheres represent iridium centers; color-code for metal hydrides (located by means of DFT calculations): blue (terminal), red (bridging) and green (semi-bridging).

Under our experimental conditions,[17] most of the iridium hydride species could be extracted from the glycerol/H_2O phase with CH_2Cl_2; however, all crystallization attempts resulted in isolation of the previously reported 'bow-tie' cluster **2**.[17] Slight modification of the reaction conditions (24h, 120 ˚C, 0.27 mL of a 1.25:1 mixture of glycerol/H_2O, 40 eq. KOH relative to **1**) allowed the isolation of a new cluster (**3** in Figure 1) after CH_2Cl_2 extraction of the crude mixture and precipitation with pentane (see Experimental Section). Based on ^1H NMR data, this cluster features 7 NHCs and 10 hydrides

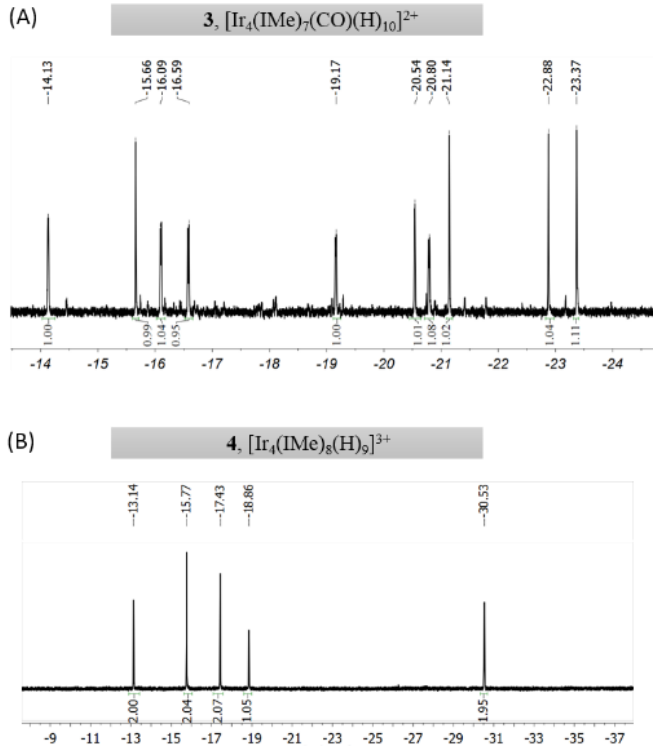

Figure 2. Hydridic region of the ^1H NMR spectra of clusters **3** and **4**

(with peaks between -14 and -24 ppm; Figure 2A). Variable temperature ^1H NMR experiments indicate that one of the NHC ligands is fluxional, with a rotation barrier of $\Delta G^{\ddagger}_{298K}$ = 14.5 kcal mol^{-1} (See ESI). The molecular formula of **3**, ($[Ir_4(IMe)_7(CO)H_{10}]^{2+}$), was determined by high-resolution MS (FT-ICR, m/z = 740.2012 (2+)) and its appropriate isotopic distribution. FT-IR spectroscopy revealed bands at 1991 and 1935 cm^{-1} assigned to Ir-CO with vibrational coupling to the hydrides. Remarkably, ^1H NMR analysis of the residual aqueous phase after CH_2Cl_2 extraction displayed a hydridic region showing a single iridium cluster species, **4** (Figure 1). This compound contains 8 NHCs and nine metal hydrides, the latter giving five distinct ^1H NMR signals in the range -13 to -31 ppm in a 2:2:2:1:2 ratio (Figure 2B). The high hydride content of clusters **3** and **4**[18] (10 and 9 hydrides, respectively) is remarkable given their high temperature synthesis in the absence of free H_2.

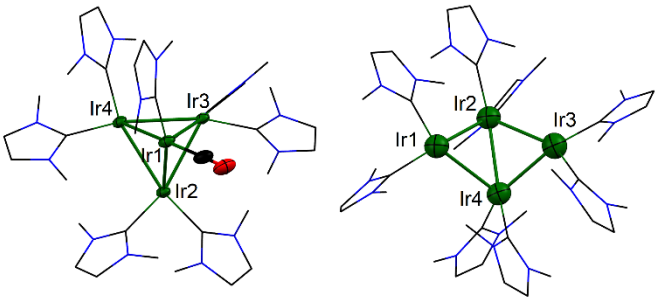

Figure 3. ORTEP diagrams of the cationic portions of compounds **3** (left) and **4** (right). 50% thermal ellipsoids are shown. For the sake of clarity hydrogen atoms have been omitted and NHC ligands displayed in wireframe style.

All attempts to obtain crystals of **3** and **4** using conventional methods were unsuccessful, in the case of **4** partly due to the presence of abundant glycerol, lactate and other polar organic catalytic side products. Nevertheless, upon adding small amounts of the polyoxometalate (POM) $[PW_{12}O_{40}]^{3-}$ to aqueous solutions of **4,** we observed that some precipitate appeared owing to the formation of an intercluster compound (**4-POM**). However, initial attempts to obtain suitable crystals of **4-POM** for X-Ray studies failed due to its insolubility. We then turned to gels as crystallization matrices (**3**: polyethylene oxide (PEO), dichloromethane/benzene; **4**: aqueous agarose, counterdiffusion with polyoxometalate), and only then were we able to grow small crystals of both clusters suitable for X-Ray analysis (Figure 3). While crystals of **3** were obtained as the BAr^F_4 (BAr^F_4 = $[B[3,5\text{-}(CF_3)_2C_6H_3]_4]^-$) salt of the cluster, in the case of **4** only the specific polyoxometalate counteranion ($[PW_{12}O_{40}]^{3-}$) was successful and provided an interesting iridium intercluster structure (**4-POM**).

The iridium cores in structures **3** and **4** differ considerably: While **3** has an almost ideal Ir_4 tetrahedral configuration ($d_{Ir\text{-}Ir}$ from 3.00 to 3.09 Å; Ir-Ir-Ir *ca.* 60°), **4** has one open edge to give a 'butterfly' Ir_4 core. Theoretical studies discussed below show the presence of two short iridium-iridium distances in **4** ($d_{Ir1\text{-}Ir2}$ = 2.741 and $d_{Ir3\text{-}Ir4}$ = 2.693 Å). The geometric parameters of **4** are also comparable to the two previous phosphine based Ir_4 'butterfly' structures.[10] The high number of NHCs, a result

of their slim steric bulk, equals that in our prior 'bow-tie' structure[17] and is promising for future exploration of NHC-rich clusters.[19] Both **3** and **4** are EAN clusters with overall electron counts of 60 and 58 electrons, respectively.[20] Compound **3** is related to **4** by formal replacement of an NHC by a carbonyl ligand and a metal hydride, which might occur through reductive elimination of imidazolium[21] ion followed by oxidative addition of H_2 (from glycerol dehydrogenation) and CO coordination (from glyceraldehyde decarbonylation).

Computational Studies

Metal hydrides in **3** and **4** could not be located in the X-Ray difference electron density map. To resolve their positions and obtain an understanding of the cluster electronic structures, **3** and **4** were optimized in the gas phase at the DFT(ωB97xd/LANL2TZ(f),6-311G**) level (see Computational Details). In these calculations, the positions of all atoms, including the hydrides and all other heavier elements, are fully optimized. The final hydride positions hereby reported are the optimal at this level of theory; *i.e.*, they yield the lowest energy. Alternative positions yield higher energies and different structures, which, for the heavy elements, deviate more from the available X-Ray data (*vide supra*). As in the crystal structure, the fully optimized geometry of the $[Ir_4(IMe)_7(CO)H_{10}]^{2+}$ cation (**3**) is based on a tetrahedral Ir_4 core (Figures 4 and S2). The distribution of the hydrides is consistent with this symmetry, also observed by NMR spectroscopy and X-Ray diffraction; *i.e.*, there are four terminal H, one for each Ir vertex, and six bridging H, one for each Ir-Ir edge. The DFT geometry is in excellent agreement with the X-Ray structure, with low minimum, maximum and root-mean square deviations (RMSD) of 0.000, 0.021 and 0.012 Å, respectively (Table S1). The Ir-H bond distances are 1.56-1.60 Å for the terminal hydrides, and 1.70-1.82 Å for the bridging ones (Table 1). The electronic structure was explored by means of natural bond orbital analysis (NBO) and non-covalent interaction plots (NCIPLOT). The natural charges found by NBO analysis are less negative on the terminal hydrides (from –0.04 to –0.10 *a.u.*) than on the bridging ones (–0.14 to –0.20 *a.u.*). Natural localized molecular orbitals (NLMOs) show that the latter are involved in *3c2e* Ir-H-Ir bonds (Figures 5 and S6) with strong d_{z^2}(Ir) ← σ(H) → d_{z^2}(Ir) donor-acceptor interactions (see SI). Further, the NCIPLOT calculations reveal the presence of attractive $H^{\delta+}$(IMe)···$H^{\delta-}$(Ir_4H_{10}) interactions as well as weak CH-π interactions between the IMe and CO ligands (Figures 6 and S7).

The $[Ir_4(IMe)_8H_9]^{3+}$ cation (**4**) was investigated at the same level of theory. Four different structural guesses based on square pyramidal and octahedral Ir(III) 18VE centers (Figure S3) all converged to the geometry shown in Figure 4. Unlike **3**, **4** has three different types of M-H bond distances (Table 1) varying from 1.550 Å (terminal) to 2.091 Å (semi-bridging, *i.e.* Ir1-H2 and I3-H7), with intermediate bridging values from 1.673 to 1.814 Å.

The natural charges found for **4** by NBO analysis are almost neutral for the terminal hydrides (0.05 *a.u.*) and negative for the bridging and semi-bridging ones (from –0.18 to –0.13 *a.u.*). Similar to **3**, bridging hydrides are involved in *3c2e* Ir-H-Ir bonds with NLMOs consisting of strong d_{z^2}(Ir) ← σ(H) → d_{z^2}(Ir) donor-acceptor interactions (Figure 5). Interestingly, the semi-bridging hydrides are also involved in *3c2e* Ir-H-Ir bonds, which involve weaker donation from σ(Ir-H) to σ*(Ir-H) orbitals (Figure S4). The NCIPLOT of $[Ir_4(IMe)_8H_9]^{3+}$ (Figures 6 and S5) shows that in analogy to **3**, the crystal is stabilized by attractive non-covalent interactions between the negatively charged bridging hydrides and the positively charged hydrogens of the methyl groups in the IMe ligands.

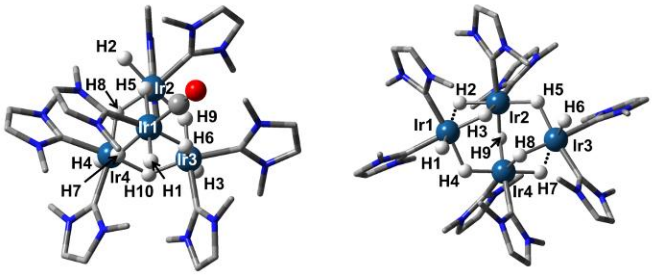

Figure 4. Gas phase optimized structures of **3** (left) and **4** (right), with the hydride positions resolved at the DFT(ωB97xd/LANL2TZ(f),6-311G**) level.

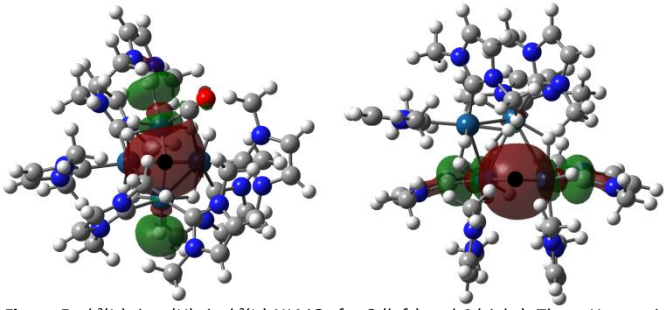

Figure 5. d_{z^2}(Ir) ← σ (H) → d_{z^2}(Ir) NLMOs for **3** (left) and **4** (right). The μ-H atom in each NLMO is highlighted in black. For more details on the NBO calculations, including stabilization energies from 2nd order perturbation analysis, see the SI.

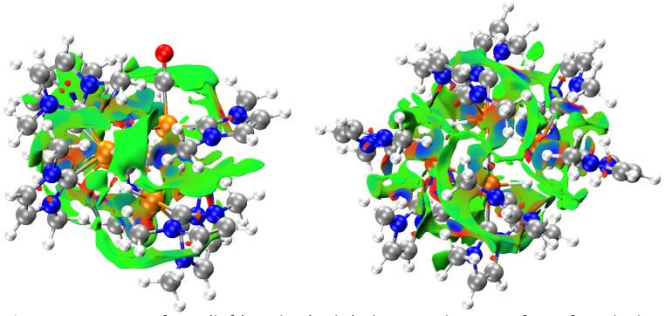

Figure 6. NCIPLOT for **3** (left) and **4** (right) showing the isosurfaces for which ρ, ∇ρ → 0 (ρ = electron density). Color code = green (weak interactions, *e.g.* CH-π) and blue (strong interactions, *e.g.* $H^{\delta+}$···$H^{\delta-}$). See the SI for more details.

Table 1. Ir-H distances at the DFT(ωB97xd/LANL2TZ(f),6-311G**) level, in Å. Atomic labels are given in Figure 4.

d(Ir-H)	Complex **3**	d(Ir-H)	Complex **4**
Ir1-H1	1.593	Ir1-H1	1.550
Ir2-H2	1.593	Ir1-H2	2.091
Ir3-H3	1.573	Ir1-H3	1.785
Ir4-H4	1.583	Ir1-H4	1.814
Ir1-H5	1.769	Ir2-H2	1.673
Ir2-H5	1.741	Ir2-H3	1.768
Ir1-H6	1.716	Ir2-H5	1.734
Ir3-H6	1.812	Ir2-H9	1.748
Ir1-H7	1.729	Ir3-H5	1.814
Ir4-H7	1.775	Ir3-H6	1.550
Ir2-H8	1.728	Ir3-H7	2.091
Ir4-H8	1.740	Ir3-H8	1.785
Ir2-H9	1.776	Ir4-H4	1.734
Ir3-H9	1.721	Ir4-H7	1.673
Ir3-H10	1.732	Ir4-H8	1.768
Ir4-H10	1.728	Ir4-H9	1.748

The DFT-optimized geometry of **4** is in good agreement with the X-Ray structure of the $Ir_4(IMe)_8$ core (Table S1). Most deviations in the Ir-Ir and Ir-C distances are <0.08 Å and the overall RMSD is 0.073 Å. These deviations may in part be caused by the absence of the counteranion in the calculations. In line with this, the largest deviation, 0.169 Å for the Ir(1)-C(2) bond length, is located in the region closest to the 3+/3– ion contact. In the X-Ray structure, this interatomic distance yields the largest deviation from the average of the Ir-C distances. Since the optimization of a 3+ charged system in gas phase may introduce geometric artefacts, the $[Ir_4(IMe)_8H_9]^{3+}$ complex was also fully optimized in diethylether with a continuum model (SMD; ε = 4.24). Remarkably, the solvated structure is not significantly different from the gas-phase one (RMSD = 0.029 Å; Table S2), probably due to the rather large size of this system (133 atoms).

Solid-state structure of 4-POM

The 'butterfly' complex **4** was crystallized as an intercluster structure containing the Keggin anion $[PW_{12}O_{40}]^3$. **4-POM** displays a rich pattern of weak interactions that, along with the Coulombic 3+/3- attractive forces, holds the two types of clusters together. Each iridium cluster is connected to four adjacent ones by means of CH-π interactions between the NHC ligands (Figure 7A) giving rise to corrugated *ac* layers. These layers are interconnected by the POM clusters along the *b*-axis following a regular stacking pattern (Figure 7C). An initial analysis shows weak C-H···O contacts connecting sp^2 and sp^3 CH groups with bridging and terminal oxygen atoms of the POMs (Figure 7B).[20] In particular, each POM cluster has seven weak to moderate C-H···O hydrogen bonding interactions with NHCs of four independent 'butterfly' clusters. These are characterized by $d_{H\cdots O}$ distances ranging from 2.41(8) to 2.49(6) Å; $d_{C\cdots O}$ from 3.10(6) to 3.32(8) Å; and C-H···O angles between 121(7) and 163(9)°. This extended set of non-covalent interactions is likely responsible for the absence of a typical 'AB' ionic packing, otherwise anticipated for the crystal lattice of a 3+/3- structure where Coulombic interactions are expected to play a pivotal role.[23]

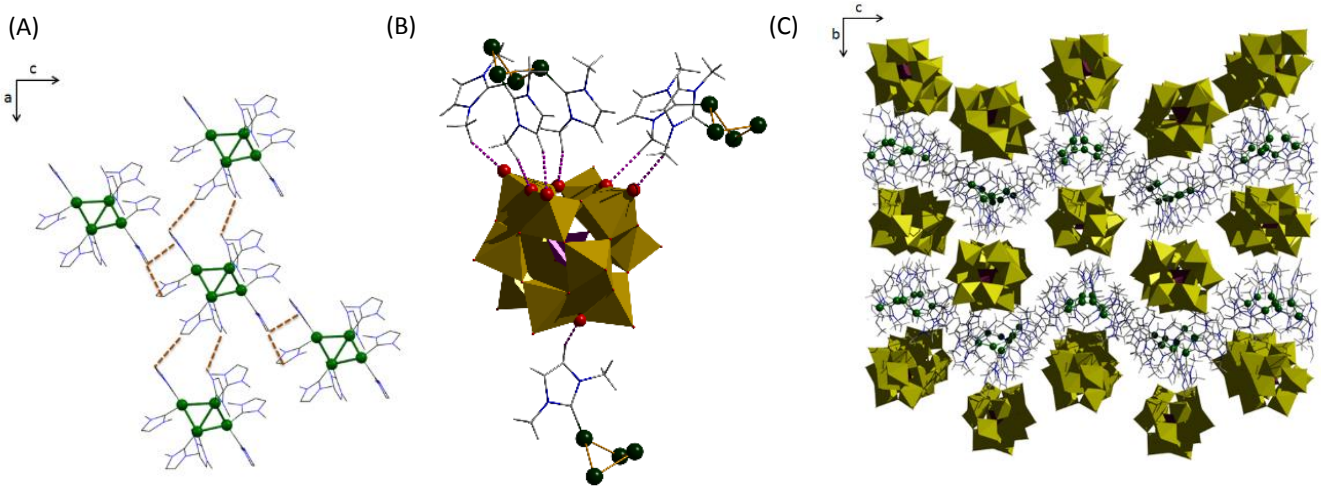

Figure 7. (A) Intermolecular weak C-H/π interactions (brown dotted lines) between NHC ligands in **4-POM**. (B) Weak C-H···O interactions between NHC ligands of Ir_4 clusters and POM. NHC ligands that do not interact with the selected POM have been omitted for clarity. (C) Projection of the crystal structure of **4-POM** along [1 0 0] with POM anions in polyhedral representation.

Interestingly, **4-POM** contains two different 1D-channels oriented along the *a*-axis (Figure 8 and Figure S8) and characterized by a cross sectional area of 5.45 x 1.28 and 5.19 x 2.65 Å^2, respectively,[24] estimated by excluding van der Waals radii from the closest H···H and O···O distances in the channels. The voids account for 21% of the total crystal volume[25] and seem to be occupied by disordered water molecules (~81 molecules per unit cell[26]) whose positions could not be determined by X-Ray studies.

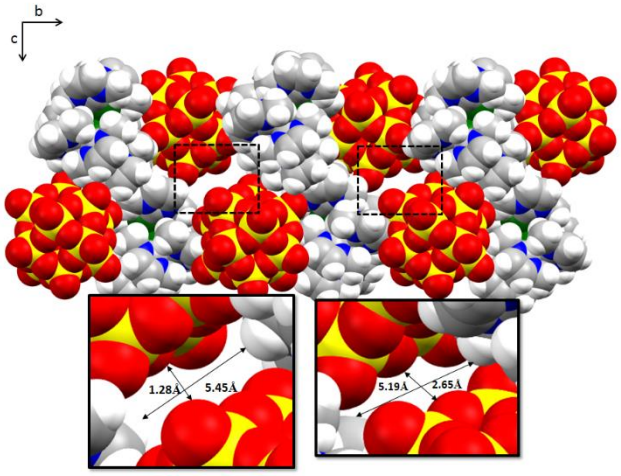

Figure 8. Space-filling model of 4-POM with a magnified view of the two cavities along [1 0 0] (color code: POM: red (oxygen), yellow (tungsten); Ir_4: green (iridium), blue (nitrogen), grey (carbon), white (hydrogen))

Conclusions

In summary, two new Ir_4 clusters with tetrahedron and 'butterfly' cores have been isolated during catalytic glycerol dehydrogenation-isomerization. X-Ray structure determination was only possible after crystallization using either aqueous (agarose, **4-POM**) or organic (polyethyleneoxide, **3**) gels, evidencing the high potential of using gel matrices for difficult crystallizations of small molecules or clusters. The crystal packing of intercluster **4-POM** is also discussed. The hydride positions for **3** and **4** were found by means of DFT calculations, which were also used to map a number of attractive non-covalent interactions between hydrides and methyl wingtips. The unusually high NHC-content of **3** and **4** is promoted by the slim sterics of IMe when compared to other bulky NHCs typically employed in catalysis. These findings could lay the groundwork for further study of unusual NHC-rich metal clusters.

Experimental Section

General

Organic solvents were pretreated by passing over activated alumina with dry N_2. All chemicals were purchased from major commercial suppliers and used as received. Syntheses of iridium complexes were performed under an inert atmosphere of dry N_2 using standard Schlenk techniques. NMR spectra were recorded on Agilent DD2-400, -500, -600 or Bruker AMX-500 spectrometers at ambient probe temperatures. Chemical shifts are reported with respect to residual internal protio solvent for ^{1}H and ^{13}C{^{1}H} NMR spectra. The chemical shift δ is reported in units of parts per million (ppm). MS analyses were performed by the Mass Spectrometry and Proteomics Resource of the W.M. Keck Foundation Biotechnology Resource Laboratory at Yale University. FT-IR spectra were recorded in a Thermo Nicolet 6700 equipped with a diamond ATR cell. Compound **1** was synthesized by a previously reported procedure.[16]

Synthesis of cluster 3 $[Ir_4(IMe)_7(CO)H_{10}][BAr^F_4]_2$

To a 0.5-2 mL biotage microwave vial equipped with a stir bar were added 15 mg $[Ir(IMe)_2(cod)]BF_4$ (**1**) and 63 mg KOH. The vial was evacuated and charged with N_2, and 0.270 mL of a degassed 1.25:1 glycerol:water solution, then sealed and heated at 120 ˚C in an oil bath for 24 hours. After cooling to room temperature, the reaction mixture was extracted with 2 x 5 mL dichloromethane, and the extract was evaporated. The resulting yellow/brown oil was dissolved in dichloromethane and precipitated with pentane 1-2 times to give $[Ir_4(IMe)_7(CO)H_{10}][BF_4]_2$ (yields varied between 10 and 25%). Near-quantitative formation of the BAr^F_4 salt was accomplished by vigorously stirring the BF_4 complex in a dichloromethane solution containing 2.1 equivalents of $NaBAr^F_4$ for 2 hours, filtering through a PTFE filter, and removing the solvent *in vacuo*. ^{1}H NMR (500 MHz, -40 ˚C, CD_2Cl_2): δ = 7.17 (br., 1H, CH_{Ar}) 6.97 (d, 1H, $^3J_{HH}$ = 2.0 Hz, CH_{Ar}), 6.88 (d, 1H, $^3J_{HH}$ = 2.0 Hz, CH_{Ar}), 6.87 (d, 1H, $^3J_{HH}$ = 2.0 Hz, CH_{Ar}), 6.84-6.86 (m, 4H, CH_{Ar}), 6.81 (d, 1H, $^3J_{HH}$ = 1.9 Hz, CH_{Ar}), 6.77 (d, 1H, $^3J_{HH}$ = 1.9 Hz, CH_{Ar}), 6.74 (d, 1H, $^3J_{HH}$ = 1.9 Hz, CH_{Ar}), 6.65 (d, 1H, $^3J_{HH}$ = 2.0 Hz, CH_{Ar}), 6.59-6.61 (m, 2H, CH_{Ar}), 4.20 (s, 3H, NMe), 3.84 (s, 3H, NMe), 3.72 (s, 3H, NMe), 3.32 (s, 3H, NMe), 3.15 (s, 3H, NMe), 3.10 (s, 3H, NMe), 3.07 (s, 3H, NMe), 2.97 (s, 3H, NMe), 2.94 (s, 3H, NMe), 2.91 (s, 3H, NMe), 2.85 (s, 3H, NMe), 2.80 (s, 3H, NMe), 2.38 (s, 3H, NMe), 1.98 (s, 3H, NMe), -14.11 (s, Ir-H), -15.65 (s, Ir-H), -15.90 (d, $^2J_{HH}$ = 6.7 Hz, Ir-H), -16.40 (d, $^2J_{HH}$ = 7.9 Hz, Ir-H), -19.20 (d, $^2J_{HH}$ = 6.7 Hz, Ir-H), -20.51 (d, $^2J_{HH}$ = 4.5 Hz, Ir-H), -20.79 (d, $^2J_{HH}$ = 7.9 Hz Ir-H), -21.25 (s, Ir-H), -22.85 (s, Ir-H), -23.35 (s, Ir-H). ^{13}C{^{1}H} NMR (150 MHz, -40 ˚C, CD_2Cl_2): δ = 180.2 (CO), 155.6 (Ir=C), 155.0 (Ir=C), 154.5 (Ir=C), 153.8 (Ir=C), 153.4 (Ir=C), 152.3 (Ir=C), 137.7 (Ir=C), 124.1 (CH_{Ar}), 122.9 (CH_{Ar}), 122.8 (CH_{Ar}), 122.3 (CH_{Ar}), 121.3 (CH_{Ar}), 121.2 (CH_{Ar}), 120.9 (CH_{Ar}), 120.8 (CH_{Ar}), 120.6 (CH_{Ar}), 120.3 (CH_{Ar}), 120.1 (CH_{Ar}), 119.9 (CH_{Ar}), 119.2 (CH_{Ar}), 118.9 (CH_{Ar}), 50.2 (NMe), 43.7 (NMe), 43.4 (NMe), 43.3 (NMe), 43.0 (NMe), 42.7 (NMe), 42.6 (NMe), 41.1 (NMe), 41.0 (NMe), 40.5 (NMe), 40.2 (NMe),. 39.6 (NMe), 38.4 (NMe), 37.0 (NMe). FT-IR (solid): ν (CO) = 1991 cm^{-1}, 1935 cm^{-1}. HRMS (FT-ICR): calcd. for $[Ir_4ON_{14}C_{36}H_{66}]^{2+}$ (M^{2+}): 740.2019 (z = 2+) Found: m/z = 740.2012 (z = 2+).

Synthesis of cluster 4, $[Ir_4(IMe)_8H_9]^{3+}$

Compound **1** (30 mg, 0.051 mmol) and KOH (80 mg, 1.43 mmol) were placed in a pressure tube and suspended in a previously deoxygenated 1:1 mixture of H_2O/glycerol (0.8 mL)

under nitrogen. The sealed pressure tube was heated at 120 ˚C for 40 h, and after cooling and releasing the overpressure, H_2O (5 mL) and dichloromethane (5 mL) were added in air. The aqueous phase was washed with dichloromethane (2 x 5mL) and evaporated under reduced pressure. The residue was dissolved in D_2O and the yield for compound **4** (from 5 to 8%) was estimated from ^{1}H NMR spectroscopy using trimethylsiylpropionate-d_4 as internal standard. Attempts to remove organic species from the aqueous mixture (glycerol, lactic acid, ethylene glycol…) were unsuccessful; however 1D and 2D homo and heteronuclear NMR experiments gave consistent spectroscopic characterization. ^{1}H NMR (600 MHz, D_2O): δ = 7.01 (d, 2H, $^3J_{HH}$ = 2.0 Hz, CH_{Ar}), 6.88 (d, 2H, $^3J_{HH}$ = 2.0 Hz, CH_{Ar}), 6.83 (d, 2H, $^3J_{HH}$ = 2.0 Hz, CH_{Ar}), 6.76 (d, 2H, $^3J_{HH}$ = 2.0 Hz, CH_{Ar}), 6.68 (d, 2H, $^3J_{HH}$ = 2.0 Hz, CH_{Ar}), 6.59 (d, 2H, $^3J_{HH}$ = 2.0 Hz, CH_{Ar}), 6.51 (d, 2H, $^3J_{HH}$ = 2.0 Hz, CH_{Ar}), 6.50 (d, 2H, $^3J_{HH}$ = 2.0 Hz, CH_{Ar}), 3.89 (s, 3H, NMe), 3.51 (s, 3H, NMe), 3.47 (s, 3H, NMe), 3.17 (s, 3H, NMe), 2.77 (s, 3H, NMe), 2.72 (s, 3H, NMe), 2.50 (s, 3H, NMe), 2.43 (s, 3H, NMe), -13.22 (s, 2H, Ir-H), -15.95 (s, 2H, Ir-H), -17.56 (s, 2H, Ir-H), -18.98 (s, 1H, Ir-H), -30.59 (s, 2H, Ir-H). ^{13}C{^{1}H} NMR (150 MHz, D_2O): δ = 152.5 (Ir=C), 151.5 (Ir=C), 149.8 (Ir=C), 145.5 (Ir=C), 122.5 (CH_{Ar}), 122.3 (CH_{Ar}), 122.2 (CH_{Ar}), 121.2 ($2CH_{Ar}$), 121.0 (CH_{Ar}), 120.6 (CH_{Ar}), 41.6 (NMe), 40.1 (NMe), 37.7 (2 NMe), 37.5 (NMe), 36.4 (NMe), 35.5 (NMe), 35.3 (NMe).

Gel-assisted crystallization of clusters.

Cluster 3. Colorless crystals of 3 were grown by solvent diffusion in a PEO (polyethyleneoxide) gel following a modification of a reported procedure.[15a] A PEO gel was prepared in a small screw cap vial by adding 60 mg PEO (MW = 1,000,000) to a 1 mL solution of 3 and sonicating vigorously. A second PEO gel was prepared by vigorously mixing 120 mg PEO with 2 mL benzene, and then layered onto the first gel. The vial was sealed, stored in the freezer where crystals were formed after one week.

Cluster 4. Agarose (25 mg) was suspended in H_2O (5mL) and the mixture heated at 90 ˚C until complete dissolution of the polysaccharide. The solution was poured into a U-tube and allowed to cool and form the gel. The vertical reservoirs were filled with the corresponding aqueous solutions of cluster 4 (3 mg) and polyoxometalate $Na_3[PW_{12}O_{40}]$ (0.3 mL, 0.01M). The reservoirs were sealed and the formation of crystals visually monitored. After three weeks small flower shaped crystals were grown and manually separated from the gel.

Crystallographic details

Low-temperature diffraction data (ω scans) were collected on a Rigaku R-AXIS RAPID diffractometer coupled to a RAXIS RAPID imaging plate detector with Mo Kα radiation (λ = 0.71073 Å) at 150K using filtered Mo Kα radiation (λ = 0.71073 Å) at 223K. The data frames were processed and scaled using the Rigaku *CrystalClear*[27] software. The data were corrected for Lorentz and polarization effects. Both structures were solved by direct methods using SHELXS-2013 or SHELXT-2014 and refined against F^2 on all data by full-matrix least squares with SHELXL-2014.[28] All non-hydrogen atoms were refined anisotropically. All hydrogen atoms were included into the model at geometrically calculated positions and refined using a riding model, except for those bound to iridium which could not be located in the Fourier difference electron density map due to the close proximity of the heavy iridium centers. The isotropic displacement parameters of all hydrogen atoms were fixed to 1.2 times the U value of the atoms to which they are linked (1.5 times for methyl groups). In structure **3** the terminal CF_3 groups of the BAr^F_4 counter ions were particularly disordered. All sets of disordered CF3 groups were refined with restraints that linked them to their respective carbon atoms. Some of the C-F distances were restrained to be similar. Structures **3** and **4** contain accessible voids with solvent molecules (0.5 C_6H_6 and 81 H_2O molecules per unit cell in **3** and **4**, respectively) that were treated as diffuse contribution to the overall scattering without specific atom positions by SQUEEZE/PLATON. Complete details of the X-ray analyses reported herein have been deposited at The Cambridge Crystallographic Data Centre (CCDC 1410898 (**3**) and CCDC 1410899 (**4**)).

Computational Details

Calculations were carried out at the DFT level by using the ωB97xd functional[29] as implemented in Gaussian09.[30] This functional, which includes both dispersion and long-range corrections, outperformed PBE0, B3LYP, B3LYP-D3 and M11 when comparing DFT-optimized geometries with X-Ray structures of similar polyhydride iridium clusters.[17] All elements were described with a triple-ζ quality basis set including polarization functions (6-311G** for C, O, N and H) and quasi-relativistic small-core pseudopotentials (LANL2TZ(f) for Ir).[31] Initial geometries were generated from the crystal structures by excluding counteranion and solvent molecules. These guesses were thereafter fully optimized without any geometry or symmetry constraint. The optimization of the 'butterfly' complex in diethylether (ε = 4.24) was performed by using the continuum SMD model.[32] Covalent bonding and non-covalent interactions were explored by means of NBO[33] (natural bond orbital analysis) and NCIPLOT[34] (non-covalent interaction plot) calculations, respectively (see ESI for further details).

Table 2 Summary of data collection, structure solution and refinement details for **3** and **4-POM**.

Compound	**3**	**4-POM**
Formula	$2(C_{32}H_{12}BF_{24})$, $C_{36}H_{56}Ir_4N_{14}$, $1.5(C6H_6)$	$C_{40}H_{74}Ir_4N_{20}$, $O_{40}PW_{12}$
Formula weight	3313.36	4495.17
T [K]	93	93
Crystal system	Triclinic	Monoclinic
Space group	P -1	P21/n
Unit cell		
a [Å]	14.6752 (3)	11.7020 (3)
b [Å]	20.0841 (5)	36.5532 (8)
c [Å]	22.7318 (16)	22.0062 (15)
α [°]	91.664 (7)	90
β [°]	107.958 (8)	96.138 (7)
γ [°]	106.800 (7)	90
V [Å^3]	6049.9 (6)	9359.1 (7)
Z	2	4
ρ_{cald} [g cm^{-3}]	1.819	3.190
μ [mm^{-1}]	4.51	37.98
F(000)	3198	7968
Crystal size [mm]	0.18 x 0.16 x 0.14	0.05 × 0.03 × 0.01
$\theta_{min} - \theta_{mac}$ [°]	3.0 – 27.5	2.0–66.2
Collected reflections	107549	223893
Indep. reflections	27634	16296
R_{int}	0.072	0.190
Completeness θ_{max}	0.996	0.986
Restraints/param.	364/1887	704/1032
GooF (F^2)	1.04	1.14
R_1, wR_2 (I>2σ(I))	0.048, 0.096	0.108, 0.309
R_1, wR_2 (all data)	0.076, 0.107	0.142, 0.335
Residual e$^-$ ρ [e Å^{-3}]	2.52/-2.03	5.20/-4.99

Acknowledgements

This work was financially supported by the CCHF, an Energy Frontier Research Center funded by the U.S. Department of Energy (DoE), Office of Science, Office of Basic Energy Sciences, under Award No. DE-SC0001298 (R.H.C. and J.C., synthesis), by the U.S. Department of Energy (DoE), Office of Science, Office of Basic Energy Sciences catalysis award (L.S., J.C., DE-FG02-84ER13297, characterization). D.B. acknowledges the support from the Norwegian Research Council through the Center of Excellence for Theoretical and Computational Chemistry (CTCC) (Grant No. 179568/V30), the Norwegian Metacenter for Computational Science (NOTUR; Grant nn4654k) and the EU Research Executive Agency for a Marie Curie Fellowship (Grant CompuWOC/618303). Dr. Pau Diaz-Gallifa is acknowledged for helpful discussions.

Notes and references

1 Metal Clusters in Chemistry, Eds.: P. Braunstein, L. A. Oro and P. R. Raithby. Wiley, New York, **1999**.

2 For recent reviews and perspectives on metal clusters see: (a) P. J. Dyson and J. S. McIndoe, *Angew. Chem. Int.* Ed., 2004, **43**, 6028; (b) P. J. Dyson and J. S. McIndoe, *Angew. Chem. Int. Ed.*, 2005, **44**, 5772; (c) G. Lavigne, *Angew. Chem. Int. Ed.,* 2012, **51**, 5794; (d) G. Hogarth, S. E. Kabir and E. Nordlander, *Dalton Trans.*, 2010, **39**, 6153.

3 L. Jin, D. S. Weinberger, M. Melaimi, C. E. Moore, A. L. Reingold and G. Bertrand, *Angew. Chem. Int. Ed*., **2014**, *53*, 9059-9063.

4 (a) L. N. Lewis, *Chem. Rev.*, 1993, **93**, 2693; (b) J. D. Grunwaldt, P. Kappen, L. Basini and B. S. Clausen, *Catal. Lett.* 2002, **78**, 13; (c) F. Li and B. C. Gates, *J. Phys. Chem. B*, 2004, **108**, 11259; (d) N. Silva, A. Solovyov and A. Katz, *Dalton Trans.*, 2010, **39**, 2194; (e) A. Uzun and B. C. Gates, *Angew. Chem., Int. Ed.*, 2008, **47**, 9245; (f) A. M. Argo, J. F. Odzak, F. S. Lai, B. C. Gates, *Nature*, 2002, **415**, 623; (g) A. Uzun and B. C. Gates, *J. Am. Chem. Soc.*, 2009, **131**, 15887.

5 (a) A. Makarem, R. Berg, F. Rominger and B. F. Straub, *Angew. Chem. Int. Ed.*, 2015, **54**, 7431-7435; (b) D. Weber and M. R. Gagné, *Org. Lett.*, 2009, **11**, 4962–4965; (c) J. L. Fulton, J. C. Linehan, T. Autrey, M. Balasubramanian, Y. S. Chen and N. K. Szymczak, *J. Am. Chem. Soc.*, 2007, **129**, 11936.

6 (a) D. Blazina, S. B. Duckett, P. J. Dyson and J. A. B. Lohman, *Angew. Chem. Int. Ed.*, 2001, **40**, 3874; (b) E. Bayram, J. C. Linehan, J. L. Fulton, J. A. S. Roberts, N. K. Szymczak, T. D. Smurthwaite, S. Ozkar, M. Balasubramanian and R. G. Finke, *J. Am. Chem. Soc.*, 2011, **133**, 18889; (c) R. Rousseau, G. K. Schenter, J. L. Fulton, J. C. Linehan, M. H. Engelhard and T. Autrey, *J. Am. Chem. Soc.*, 2009, **131**, 10516–10524.

7 R. H. Crabtree, *Chem. Rev.*, 2015, **115**, 127.

8 S. P. Smidt, A. Pfaltz, E. Martinez-Viviente, P. S. Pregosin, A. Albinati, *Organometallics* 2003, **22**, 1000.

9 (a) D. F. Chodosh, R. H. Crabtree, H. Felkin, S. Morehouse and G. E. Morris, *Inorg. Chem.*, 1982, **21**, 1307; (b) H. H.Wang and L. H. Pignolet, *Inorg. Chem.*, 1980, **19**, 1470; (c) A. L. Casal, L. H. Pignolet, J. W. A. van der Velden, J. J. Bour and J. J. Steggerda, *J. Am. Chem. Soc.*, 1983, **105**, 5957; (d) H. H. Wang, A. L. Casalnuovo, B. J. Johnson, A. M. Mueting, L. H. Pignolet, *Inorg. Chem.*, 1988, **27**, 325; (e) S. P. Smidt, A. Pfaltz, E. Martinez-Viviente, P. S. Pregosin and A. Albinati, *Organometallics*, 2003, **22**, 1000.

10 Y. Xu, M. A. Celik, A. L. Thompson, H. Cai, M. Yurtsever, B. Odell, J. C. Green, D. M. P. Mingos, and J. M. Brown *Angew. Chem. Int. Ed.*, 2009, **48**, 582.

11 L. S. Sharninghausen, J. Campos, M. G. Manas and R. H. Crabtree, *Nat. Commun.*, 2014, **5**, 5084.

12 (a) M. C. Robert and F. Lefaucheux, *J. Cryst. Growth.*, 1988, **90**, 358; (b) J. M. García-Ruiz, *Key Eng. Mat.* 1991, **58**, 87.

13 (a) Crystals in Gels and Liesegang Rings. Ed. H. K. Henisch. Cambridge University Press: Cambridge, 1988; (b) Crystallization in gels and related methods. M. C. Robert, O. Vidal, J. M. García-Ruiz and F. Otálora. In Crystallization of nucleic acids and proteins: A practical approach, Eds. A. Ducruix and R. Giegé, Oxford University Press: New York, 1999.

14 (a) Protein Crystallization (Ed.: T. M. Bergfors), Internat'l University Line, 2009. (b) Crystallization of Biological Macromolecules (Ed.: Alexander McPherson), Cold Spring Harbor Laboratory Press, 1999. (c) Macromolecular Crystallization and Crystal Perfection (N. E Chayen, J. R Helliwell and E. H Snell), OUP Oxford, 2010.

15 See for example: (a) D. Choquesillo-Lazarte and J. M. Garcia-Ruiz, *J. Appl. Cryst.*, 2011, **44**, 172; (b) I. Tsyba, B. B. K. Mui, R. Bau, R. Noguchi and K. Nomiya, *Inorg. Chem.*, 2003, **42**, 8028; (c) J. M. Bravo-Arredondo, A. Moreno and M. E. Mendoza, *J. Cryst. Growth,* 2014, **401**, 242; (d) S. N. Kalkura and S. Devanarayanan, J. Cryst. Growth, 1991, **110**, 265; (e) R. Clérac , S. O'Kane , J. Cowen, X. Ouyang, R. Heintz, H. Zhao, M. J. Bazile and K. R. Dunbar, *Chem. Mater.*, 2003, **15** , 1840; (f) R. Andrés , M. Gruselle, B. Malézieux, M. Verdaguer and J.

Vaissermann, *Inorg. Chem.*, 1999, **38**, 4637; (g) J. H. Son, H. Choi and Y. U. Kwon, *J. Am. Chem. Soc.*, 2000, **122**, 7432.
16 (a) J. Campos, U. Hintermair, T. P. Brewster, M. K. Takase and R. H. Crabtree, *ACS Catal.*, 2014, **4**, 973. (b) U. Hintermair, J. Campos, T. P. Brewster, L. Pratt, N. D. Schley and R. H. Crabtree, *ACS Catal.*, 2014, **4**, 99.
17 J. Campos, L. S. Sharninghausen, R. H. Crabtree and D. Balcells, *Angew. Chem. Int. Ed.*, 2014, **53**, 12808.
18 For recent examples on hydride-rich metal clusters see: (a) A. S. Weller and J. S. McIndoe, *Eur. J. Inorg. Chem.*, 2007, 4411; (b) R. F. Adams and B. Captain, *Angew. Chem. Int. Ed.*, 2005, **44**, 2531; (c) R. D. Adams, B. Captain and L. Zhu, *J. Am. Chem. Soc.*, 2007, **129**, 2454; (d) S. K. Brayshaw, M. J. Ingleson, J. C. Green, J. S. McIndoe, P. R. Raithby, G. Kociok-Kohn and A. S. Weller, *J. Am. Chem. Soc.,* 2006, **128**, 6247.
19 (a) J. A. Cabeza and P. García-Álvarez, *Chem. Soc. Rev.*, 2011, **40**, 5389; (b) J. A. Cabeza, M. Damonte, P. García, M. G. Herna and A. R. Kennedy, *Organometallics*, 2012, **31**, 327.; (c) J. A. Cabeza, M. Damonte, P. García-Álvarez and E. Pérez-Carreño, *Organometallics*, 2013, **32**, 9251; (d) S. Warratz, L. Postigo and B. Royo, *Organometallics*, 2013, **32**, 893; (e) M. R. Critall, C. E. Ellul, M. F. Mahon, O. Saker and M. K. Whittlesey, *Dalton Trans.*, 2008, 4209.
20 The Organometallic Chemistry of the Transition Metals, 6th Ed.,R. H. Crabtree, John Wiley & Sons, Inc. **2014**, Chapter 2.
21 (a) C. M. Crudden and D. P. Allen, *Coord. Chem. Rev.*, 2004, **248**, 2247; (b) D. Bacciu, K. J. Cavell, I. A. Fallis and L.-I. Ooi, *Angew. Chem. Int. Ed.*, 2005, **44**, 5282; (c) D. S. McGuinness and K. J. Cavell, *Organometallics*, 2000, **19**, 4918.
22 (a) T. Steiner, *Angew. Chem. Int. Ed.*, 2002, **41**, 48. (b) M. J. Calhorda, *Chem. Commun.*, 2000, 801. (c) G. R. Desiraju, *Acc. Chem. Res.*, 1996, **29**, 441.
23 M. Schulz-Dobrick and M. Jansen, *Inorg. Chem.*, 2007, **46**, 4380.
24 L. J. Barbour, *Chem. Commun.*, 2006, 1163.
25 The void volume was calculated using the PLATON package (L. A. Spek, PLATON, A Multipurpose Crystallographic Tool; Utrecht University: Utrecht, The Netherlands, 2001).
26 The water molecules were treated as a diffuse contribution to the overall scattering without specific atom positions by the SQUEEZE program (see P. v.d. Sluis, A.L. Spek, *Acta Cryst,* 1990, **A46**, 194).
27 *CrystalClear* and *CrystalStructure*; Rigaku/MSC: The Woodlands, TX, **2005**.
28 G. M. Sheldrick, *Acta Cryst.,* 2008, **A64**, 112.
29 Chai, J.-D.; Head-Gordon, M. *Phys. Chem. Chem. Phys.*, **2008**, *10*, 6615.
30 Gaussian 09, Revision D.01, Frisch, M. J.; Trucks, G. W.; Schlegel, H. B.; Scuseria, G. E.; Robb, M. A.; Cheeseman, J. R.; Scalmani, G.; Barone, V.; Mennucci, B.; Petersson, G. A.; Nakatsuji, H.; Caricato, M.; Li, X.; Hratchian, H. P.; Izmaylov, A. F.; Bloino, J.; Zheng, G.; Sonnenberg, J. L.; Hada, M.; Ehara, M.; Toyota, K.; Fukuda, R.; Hasegawa, J.; Ishida, M.; Nakajima, T.; Honda, Y.; Kitao, O.; Nakai, H.; Vreven, T.; Montgomery, Jr., J. A.; Peralta, J. E.; Ogliaro, F.; Bearpark, M.; Heyd, J. J.; Brothers, E.; Kudin, K. N.; Staroverov, V. N.; Kobayashi, R.; Normand, J.; Raghavachari, K.; Rendell, A.; Burant, J. C.; Iyengar, S. S.; Tomasi, J.; Cossi, M.; Rega, N.; Millam, N. J.; Klene, M.; Knox, J. E.; Cross, J. B.; Bakken, V.; Adamo, C.; Jaramillo, J.; Gomperts, R.; Stratmann, R. E.; Yazyev, O.; Austin, A. J.; Cammi, R.; Pomelli, C.; Ochterski, J. W.; Martin, R. L.; Morokuma, K.; Zakrzewski, V. G.; Voth, G. A.; Salvador, P.; Dannenberg, J. J.; Dapprich, S.; Daniels, A. D.; Farkas, Ö.; Foresman, J. B.; Ortiz, J. V.; Cioslowski, J.; Fox, D. J. Gaussian, Inc., Wallingford CT, **2013**
31 (a) McLean, A. D.; Chandler, G. S. *J. Chem. Phys.*, **1980**, *72*, 5639; (b) Roy, L. E.; Hay, P. J.; Martin, R. L. *J. Chem. Theory Comput.*, **2008**, *4*, 1029.
32 Marenich, A. V.; Cramer, C. J.; Truhlar, D. G. *Phys. Chem. B*, **2009**, *113*, 6378.
33 Glendening, E. D.; Landis, C. R.; Weinhold, F. *J. Comput. Chem.*, **2013**, *16*, 1429
34 Contreras-García, J.; Johnson, J. E. R.; Keinan, S.; Chaudret, R.; Piquemal, J.-P.; Beratan, D. N.; Yang, W. *J. Chem. Theory Comput.*, **2011**, *7*, 625.

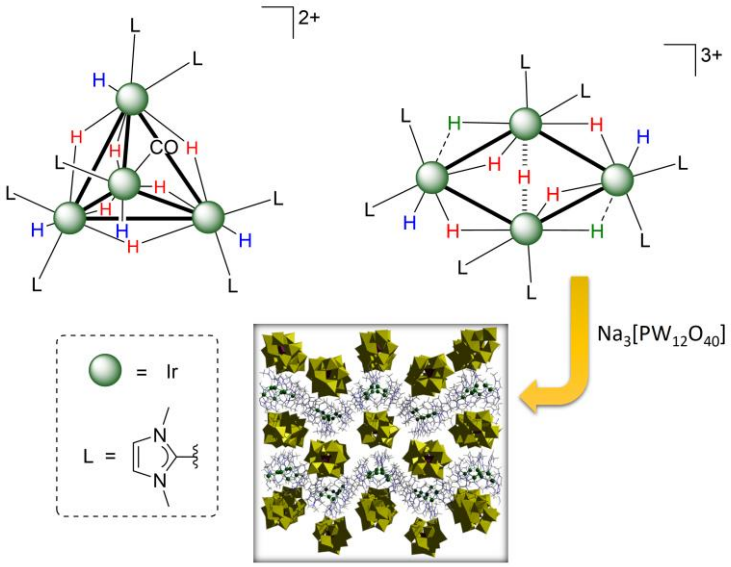

Two unique Ir_4 clusters isolated during catalytic glycerol dehydrogenation, crystallized using aqueous and organic gel matrices and displaying remarkable structural features are described.